Identification and Learning in Autonomous Vehicle Control Systems

WANG Leyi [1], George Yin[2], ZHAO Guangliang[3], LI Shengbo[4], Xu Biao[4], LI Keqiang[4]

(1. *Department of Electrical and Computer Engineering, Wayne State University,* Detroit, MI 48202, USA; 2. *Department of Mathematics, Wayne State University,* Detroit, MI 48202, USA; 3. *GE Global Research Niskayuna,* NY 12309, USA; 4. *Department of Automotive Engineering Tsinghua University,* Beijing 100084, China)

Abstract: System parameters of autonomous vehicles need to be identified and learned during operation to solve the problem that autonomous vehicles encounter many uncertainties that change with time, operating conditions, and environments. By capturing system behavior in a closed-loop setting and using data to learn the related parameters, system reliability and robustness can be quantitatively established. This paper focuses on a basic scenario of an autonomous vehicle following its front vehicle. By integrating control actions with vehicle dynamics, a learning algorithm using operational data and confidence ellipsoids was employed to support robustness and reliability. A simulation case study was used to illustrate the strategies. The results show the proposed method can estimate the vehicle's parameters accurately.

Key words: vehicle control; autonomous vehicle; identification of parameters; learning; robustness

自动驾驶汽车控制系统参数辨识与学习（英文）

王乐一[1]，殷　刚[2]，赵广亮[3]，李升波[4]，徐　彪[4]，李克强[4]

（1. 韦恩州立大学　电气与计算机工程系，底特律市 MI 48202，美国；2. 韦恩州立大学　数学系，底特律市 MI 48202，美国；3. 通用电气公司　全球科研中心，尼斯卡于纳市 MI 48202，美国；4. 清华大学　汽车工程系，北京 100084，中国）

摘　要：针对自动驾驶汽车在行驶过程中会遇到随时间和交通环境变化的不确定性，须对自动驾驶系统参数进行辨识和学习。通过获取闭环状态下的系统行为和学习数据驱动下的系统参数，可极大提升系统辨识可靠性和稳定性。本文对自动驾驶车辆跟车的典型场景，综合考虑车辆控制和动力学特性，构建了基于车辆运行数据和置信椭圆的系统参数辨识的学习算法，提升系统辨识的可靠性和鲁棒性。结果表明提出的参数辨识和学习方法可准确估计车辆参数。

关键词：汽车控制；自动驾驶车辆；参数辨识；学习；鲁棒性

中图分类号：U 495; TP 242.6; U 461.6　**文献标识码：**A　DOI: 10.3969/j.issn.1674-8484.2018.02.003

收稿日期 / Received：2017-11-17。

基金项目 / Supported by：The National Natural Science Fund Projeet / 国家自然科学基金资助项目（ 51575293、51622504）；National Key R&D Program of China（2016YFB0100906）；International Sci &Tech Cooperation Program of China (2016YFE0102200)。

第一 作者 / First author：王乐一 / WANG Leyi (1955—)，男 / male (汉族)，上海，教授。E-mail: lywang@wayne.edu。

Introduction

Autonomous driving has the potential to improve vehicle fuel economy. Especially during car-following, onboard controllers in autonomous vehicles can decrease wind resistance with smaller car-following gaps, which can significantly reduce fuel consumption. Nowadays, many studies have focused on car-following control of autonomous vehicles. For example, Xu et al presented an estimated minimum principle and kinetic energy conversion method with safety-guaranteed car-following models to realize eco-cruising on varying slopes in the car-following scenario [1]. Zheng et al introduced a distributed model predictive control (DMPC) algorithm for heterogeneous vehicle platoons with unidirectional topologies and *a priori* unknown desired set points, in which a penalty on errors between the predicted and assumed trajectories and an equality-based terminal constraint was proposed to ensure stability [2]. Li et al used a dual-pulse-and-glide method in an automated vehicle platoon by adopting a sectionalized switching map which achieves bounded stability for the homogeneous platoon, with the range error of each follower being exactly confined within a predefined central region [3].

However, autonomous vehicles encounter many uncertainties involving road conditions, vehicle interactions, and environments that change with time and operating conditions [4-8]. Dealing with these uncertainties is challenging. Some researchers tended to solve the problem by using some model-based robust controllers. For example, Gao et al presented an H^{∞} control method for a platoon of heterogeneous vehicles with uncertain vehicle dynamics and uniform communication delays, in which the requirements of string stability, robustness and tracking performance were systematically measured by the H^{∞} norm, and explicitly satisfied by casting into the linear fractional transformation format [9]. Li et al proposed a pulse-and-glide operation algorithm for an adaptive cruise control system with internal combustion engine and step-gear transmission to minimize fuel consumption in car-following scenarios [10]. To enhance the robustness against model mismatch, they introduced a bounded feedback regulator. Li et al suggested a Riccati inequality-based robust controller synthesis algorithm for vehicular platoons with bounded parameter uncertainties, whose computational complexity is independent of platoon size [11].

Other methods to deal with the uncertainties in car-following control problems is the parameter estimation method. This paper introduced a methodology that integrated vehicle control, system identification, and supervised learning to deal with uncertainties in a vehicle driving environment. Control, estimation, and learning strategies were introduced, and computationally efficient recursive algorithms were developed. Convergence properties of the algorithms were established. A learning algorithm using confidence ellipsoids was employed to support robustness and reliability. A simulation case study was used to illustrate the strategies.

1 Problem Formulation

We used a basic scenario of autonomous vehicles to motivate the study of this paper. Consider an autonomous vehicle that follows its front vehicle; see Figure 1. The front vehicle's speed v_{ref} is a reference signal that is either measured or communicated. v_{ref} may be viewed as a random process with certain statistical properties, due to lack of knowledge on the front vehicle's intention. Furthermore, the measured front distance d and vehicle speed v are subject to errors. The vehicle controller then acts on the measured signals and information about the dynamics and environment to control the vehicle's movements.

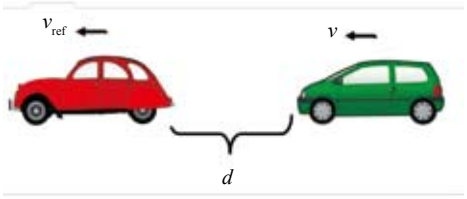

Figure 1 Autonomous Vehicles

We start with a simplified vehicle dynamics

$$\dot{d} = v_{\mathrm{ref}} - v\,,$$
$$m\dot{v} = f - c(v). \tag{1}$$

where v is the vehicle speed, m is the total mass , and f is the consolidated driving force on the center of gravity of the vehicle, $c(v)$ represents the combined resistance effect of gravitational pull, tire friction, vehicle mechanical friction, air-drag coefficient, etc. Here, we allow $c(v)$ to be a linear combination of base functions: $c(v) = a_1\, g_1\,(v)+\cdots+a_p\, g_p\,(v)$ with known base functions $g_i\,(v)$, $i = 1,\cdots, p$. One common example is $c(v) = a_0 + a_2\, v^2$ for $v > 0$.

Suppose that the actual control signal is u and the actuator dynamics are represented by a first-order system

$$\dot{f} + af = bu. \tag{2}$$

Denote $g(\dot{v}\,,v) = \mathrm{d}c(v)/\mathrm{d}t = [\mathrm{d}c(v)/\mathrm{d}v]\,\dot{v}$. It follows that

$$\begin{aligned} m\,\ddot{v} \;&= \dot{f} - g(\dot{v}\,,v) = \\ &\quad -af + bu - g(\dot{v}\,,v) = \\ &\quad -a\left[m\,\dot{v} + c(v)\right] - g(\dot{v}\,,v) + bu. \end{aligned}$$

or

$$m\,\ddot{v} + am\,\dot{v} + g(\dot{v}\,,v) + ac(v) = bu.$$

The feedback control can be designed, for example, as

$$u = \gamma_{\mathrm{d}}(d - d_{\mathrm{ref}}) + \gamma_{\mathrm{v}}(v_{\mathrm{ref}} - v).$$

Here, d_{ref} is the desired car-following distance. Since the vehicle dynamics are unknown, the model parameters must be estimated based on input-output observations of length N. Let θ be the unknown model parameter vector and its estimate be θ_N. The control parameters are designed on the basis of θ_N. This introduces a control robustness problem: The closed-

loop system's stability and performance will be affected by estimation errors.

Robustness of the controller means that it can tolerate estimation errors to a certain bound. This can be specified by a set of θ under which the controller can maintain stability and meet the design specifications. Then, control reliability can be specified as the probability that the estimation error is falling within the controller's robustness region.

Given a (small) sampling interval $\tau > 0$, we may express the sampled closed-loop system as

$$z_k = \boldsymbol{\varphi}_k^{\mathrm{T}}\boldsymbol{\theta}. \tag{3}$$

where z_k is a derived signal, φ_k^{T} is the regressor containing observed data and θ is the parameter vector to be identified or learned. Noise corrupted observations imply that both z_k and φ_k contain measurement errors whose structure depends on system details. Some nonlinear systems can be embedded into this linear regression structure since the regressor φ_k may contain some nonlinear functions of the measured signals.

Data are acquired by using noise-corrupted observations

$$z_k = \boldsymbol{\varphi}_k^{\mathrm{T}}\boldsymbol{\theta}, \quad k = 1, 2, ..., N.$$

An identification algorithm can be specified to estimate $\boldsymbol{\theta}$, leading to $\boldsymbol{\theta}_N$.

We adopt a set-based robustness characterization in this paper. Since detailed specifications on the plant and controller are highly problem specific, we assume that an estimation error set $\boldsymbol{M}$ has been specified such that if $\boldsymbol{\theta}_N - \boldsymbol{\theta} \in \boldsymbol{M}$, the design specifications will be met. The set M defines the robustness region of the controller. Since estimation of θ is performed on the basis of noise-corrupted observations, θ_N is a random process whose probability distribution depends on the identification algorithm, noise features, and the data size N.

Controller reliability is a probabilistic description of the controller's ability in meeting design specifications. For a selected confidence level $0 < \alpha < 1$, we require that the probability of meeting the design specifications be at least $1-\alpha$

$$P\{\boldsymbol{\theta}_N \in \boldsymbol{M}\} \geqslant 1 - \alpha. \tag{4}$$

This paper is focused on reliability issues in this problem. More specifically, we are interested in knowing how big the data size N needs to be so that the control reliability Eq. (4) is achieved. It is noted that this problem is closely related to stochastic stoping rules in which characterizing conditions are sought for an algorithm to stop at a finite time with guaranteed identification accuracy. This is in contrast to convergence analysis which ensures accurate estimation when data sizes go to infinity.

2 Identification and Learning

2.1 Algorithms and Convergence Analysis

Estimates of $\boldsymbol{\theta}$ in Eq. (3) can be obtained by minimizing the following mean-square errors

$$\min_{\theta} J(\boldsymbol{\theta}) = E(z_k - \boldsymbol{\varphi}_k^{\mathrm{T}}\boldsymbol{\theta})^2, \tag{5}$$

where, $\boldsymbol{\theta}, \boldsymbol{\varphi}_k \in \mathbb{R}^m$, $z_k \in \mathbb{R}^m$, and E is the expectation with respect to the underlying probability space.

By defining $\boldsymbol{\Phi} = [\boldsymbol{\varphi}_1, \boldsymbol{\varphi}_2, ..., \boldsymbol{\varphi}_N]$ and $\boldsymbol{Z} = [z_1, z_2, ..., z_k]^{\mathrm{T}}$, a gradient-based searching algorithm for Eq. (5) leads to the parameter updating algorithm

$$\boldsymbol{\theta}_{k+1} = \boldsymbol{\theta}_k - \boldsymbol{\Phi}\boldsymbol{\Phi}^{\mathrm{T}}\boldsymbol{\theta}_k + \frac{1}{k}\boldsymbol{\Phi}\boldsymbol{Z}. \tag{6}$$

Here, to be specific we have selected the updating step size $1/k$ although other selections are certainly possible. For convergence and reliability analysis, we impose the following assumptions.

(A1): $\{(\boldsymbol{\varphi}_k, z_k)\}$ is a sequence of stationary $\boldsymbol{\Phi}$-mixing process such that

$$E\boldsymbol{\varphi}_k\boldsymbol{\varphi}_k^{\mathrm{T}} = \boldsymbol{A}, \quad E\boldsymbol{\varphi}_k z_k = \boldsymbol{b}.$$

where $\boldsymbol{A}$ is a positive definite matrix with the smallest eigenvalue $\lambda_{\min}(\boldsymbol{A}) > 0.5$.

(A2): The following bound holds:

$$\sup_k E|z_k|^{4+\beta} < \infty \quad \text{for some } \beta > 0.$$

(A3): Denote $\boldsymbol{\zeta}_k = \boldsymbol{\varphi}_k \boldsymbol{z}_k - \boldsymbol{\varphi}_k\boldsymbol{\varphi}_k^{\mathrm{T}}\boldsymbol{\theta}$. Let the σ-field and its filtration be

$$\mathcal{F}_n = \sigma\{\boldsymbol{\zeta}_k; k \leqslant n\}, \ \mathcal{F}^n = \sigma\{\boldsymbol{\zeta}_k; k \geqslant n\}.$$

For m > 0, let

$$\phi(l) = \sup_{B \in \mathcal{F}^{n+l}} |P(B|\mathcal{F}_n) - P(B)|_p,$$

such that

$$\sum_l \phi(l)^{\frac{\delta}{1+\delta}} < \infty.$$

where $|z|_p$ denotes the p-norm $|z|_p = E^{\frac{1}{p}}|z|^p$, with $p = \frac{2+\delta}{1+\delta}$, and $\delta = \frac{\beta}{2}$.

Remark 1: Condition **(A1)** assumes that $\boldsymbol{A}$,$\boldsymbol{b}$ exist. In addition, $\boldsymbol{A}$ is invertible, which is essentially a "persistent excitation" condition for parameter identifiability. As a result, by the Gauss-Markov estimations [12], the optimal solution to Eq. (5) is

$$\boldsymbol{\theta}_{\mathrm{opt}} = \boldsymbol{A}^{-1}\boldsymbol{b}.$$

However, without knowledge on the probability distributions or at least the second moments $\boldsymbol{A}$ and $\boldsymbol{b}$, $\boldsymbol{\theta}_{\mathrm{opt}}$ is unknown. We are seeking algorithms that have inherent self-learning capability such that the estimates will converge to $\boldsymbol{\theta}_{\mathrm{opt}}$. In what follows, we denote $\boldsymbol{\theta}_{\mathrm{opt}}$ by $\boldsymbol{\theta}$ for simplicity.

Assumption **(A1)** also implies that the matrix $\boldsymbol{C} = 0.5\boldsymbol{I} - \boldsymbol{A}$ is negative definite and hence stable. This is useful for convergence analysis.

Assumptions **(A2)** and Assumptions **(A3)** are needed in the development of functional invariant theory. Roughly speaking, the $\boldsymbol{\Phi}$-mixing assumption tells us that the data are asymptotically independent. The $\boldsymbol{\Phi}$(l) defined above is known

as a mixing measure for the level of independence between two σ-algebras.

The following convergence analysis uses a similar approach as Ref. [13]. In that paper, a minimization problem Eq. (5) together with a constraint was considered. For the learning algorithm Eq. (6), no constraints are needed. As a result, it becomes a special case discussed in Ref. [13]. We present the result below and omit its proof.

Proposition 1: Under **(A1)** ~ **(A3)**, the supervised learning algorithm (6) is strongly consistent, i.e., $\boldsymbol{\theta}_k \to \boldsymbol{\theta}$ a.s., as $k \to \infty$.

2.2 Robustness and Reliability of Control Strategies

In this paper, we allow a wide variety of control strategies, but impose the following requirements: The control strategy leads to satisfactory performance robustly if the parameter estimate $\boldsymbol{\theta}_k$ satisfies $\|\boldsymbol{\theta}_k - \boldsymbol{\theta}\| \leqslant \epsilon$ for some $\epsilon > 0$ under a selected norm $\|\cdot\|$. This is a robustness condition on the control strategy.

However, since $\boldsymbol{\theta}_k$ is a random variable, the robustness condition $\|\boldsymbol{\theta}_k - \boldsymbol{\theta}\| \leqslant \epsilon$ is an event in the corresponding probability space. This leads to a probabilistic characterization of the reliability on the control strategy.

Let α be a selected confidence level. We wish to characterize a region of $\boldsymbol{\theta}_k$ (a stopping rule) such that $P\{\|\boldsymbol{\theta}_k - \boldsymbol{\theta}\| \leqslant \epsilon\} \geqslant 1-\alpha$. This implies that the stopping rule relies on a clear characterization of the corresponding confidence region. Unfortunately, since the underling probability information is not available and the accurate shape to the confidence region can be extremely difficult to describe, it is nearly impossible to build the accurate confidence region. We seek approximate descriptions of confidence regions in the next subsection.

2.3 Asymptotic Normality

An early approach of approximate confidence regions was proposed in [14] and then employed in our previous work [15-16]. The essential idea is based upon the asymptotic normality of a stopped stochastic process. The approximate confidence region we shall be building is a confidence ellipsoid.

The procedure can be briefly described as follows. Denote by x^2_{m} the Chi-square distribution with m degrees of freedom. Choose a desired estimation error (or neighborhood size) ϵ, pick up a confidence level α and a number c_α, such that

$\lim_{\epsilon \to 0} P$ {the confidence ellipsoid with volume $\leqslant \epsilon^m$ covers $\boldsymbol{\theta}_k$ } = $P\{x^2_{\mathrm{m}} \geqslant c_\alpha\}$=1-$\alpha$.

The asymptotic normality is crucial in the subsequent development. We first recall an important result. Let

$$\psi(k|j) = \begin{cases} \prod_{l=j+1}^{k} \left(\boldsymbol{I} - \frac{\boldsymbol{A}}{l}\right), k \geqslant j+1, \\ \boldsymbol{I}, k = j. \end{cases}$$

Then

$$\boldsymbol{\theta}_{k+1} = \psi(k|1)(\boldsymbol{\theta}_1 - \boldsymbol{\theta}) + \sum_{l=1}^{k} \frac{1}{l} \psi(k|l)\boldsymbol{\zeta}_l + \sum_{l=1}^{k} \frac{1}{l} \psi(k|l)\left(\boldsymbol{A} - \boldsymbol{y}_l \boldsymbol{y}_l^{\mathrm{T}}\right)(\boldsymbol{\theta}_l - \boldsymbol{\theta}),$$

We claim that

$$\sqrt{k}\,\psi(k|1)(\boldsymbol{\theta}_1 - \boldsymbol{\theta}) + \sqrt{k} \sum_{l=1}^{k} \frac{1}{l} \psi(k|l)\left(\boldsymbol{A} - \boldsymbol{y}_l \boldsymbol{y}_l^{\mathrm{T}}\right)(\boldsymbol{\theta}_l - \boldsymbol{\theta}) = o(1),$$

Where, $o(1) \to 0$ in probability as $k \to \infty$. To see this, we observe that

$$\sqrt{k}\,|\psi(k|1)(\boldsymbol{\theta}_1 - \boldsymbol{\theta})| \leqslant K k^{-\lambda_{\min}(\boldsymbol{A})+0.5}.$$

Since $\lambda_{\min}(\boldsymbol{A}) > 0.5$, the above quantity tends to 0 as $k \to \infty$ a.s.

We note that by the strong consistency, for any $\eta > 0$, there exists $\boldsymbol{M} > 0$ such that for all $k \geqslant \boldsymbol{M}$, $|\overline{\boldsymbol{S}}_k - \overline{\boldsymbol{S}}| < \eta$. Now write the second term as

$$\sqrt{k} \sum_{l=1}^{k} \frac{1}{l} \psi(k|l)\left(\boldsymbol{A} - \boldsymbol{y}_l \boldsymbol{y}_l^{\mathrm{T}}\right)(\boldsymbol{\theta}_l - \boldsymbol{\theta}) =$$

$$\sqrt{k} \sum_{l=1}^{M-1} \frac{1}{l} \psi(k|l)\left(\boldsymbol{A} - \boldsymbol{y}_l \boldsymbol{y}_l^{\mathrm{T}}\right)(\boldsymbol{\theta}_l - \boldsymbol{\theta}) +$$

$$\sqrt{k} \sum_{l=M}^{k} \frac{1}{l} \psi(k|l)\left(\boldsymbol{A} - \boldsymbol{y}_l \boldsymbol{y}_l^{\mathrm{T}}\right)(\boldsymbol{\theta}_l - \boldsymbol{\theta}).$$

The first term above can be shown to converge to 0 a.s. We now show that the second term converges in the mean to 0. It follows that

$$E\left|\sqrt{k} \sum_{l=M}^{k} \frac{1}{l} \psi(k|l)\left(\boldsymbol{A} - \boldsymbol{y}_l \boldsymbol{y}_l^{\mathrm{T}}\right)(\boldsymbol{\theta}_l - \boldsymbol{\theta})\right| \leqslant$$

$$K\eta\sqrt{k} \sum_{l=M}^{k} \frac{1}{l} \psi(k|l)^{\lambda_{\min}(\boldsymbol{A})} \left\{E\left|\boldsymbol{A} - E_M \boldsymbol{y}_l \boldsymbol{y}_l^{\mathrm{T}}\right| E\left|E_M \boldsymbol{y}_l \boldsymbol{y}_l^{\mathrm{T}} - \boldsymbol{y}_l \boldsymbol{y}_l^{\mathrm{T}}\right|\right\} \leqslant$$

$$K\eta \sum_{l=M}^{k} \phi^{\frac{\delta}{1+\delta}} (l - \boldsymbol{M}) E^{\frac{1}{2+\delta}} |\boldsymbol{y}_M|^{2+\delta} \leqslant K\eta,$$

where E_M denotes the conditional expectation on F_M.

In the above, we have used an argument from [17],

$$E\left|\boldsymbol{A} - E_M \boldsymbol{y}_l \boldsymbol{y}_l^{\mathrm{T}}\right| \leqslant K\phi^{\frac{\delta}{1+\delta}} (\boldsymbol{l} - \boldsymbol{M}) E^{\frac{1}{2+\delta}} |\boldsymbol{y}_M|^{2+\delta},$$

$$E\left|E_M \boldsymbol{y}_l \boldsymbol{y}_l^{\mathrm{T}} - \boldsymbol{y}_l \boldsymbol{y}_l^{\mathrm{T}}\right| \leqslant K\phi^{\frac{\delta}{1+\delta}} (\boldsymbol{l} - \boldsymbol{M}) E^{\frac{1}{2+\delta}} |\boldsymbol{y}_M|^{2+\delta}.$$

The above assertion implies that to study the asymptotic distribution of $\sqrt{k}(\boldsymbol{\theta}_{k+1} - \boldsymbol{\theta})$, we need only consider $\sqrt{k}\sum_{l=1}^{k} \frac{1}{l} \psi(k|l)\boldsymbol{\zeta}_l$.

3 Approximate Confidence Regions

Define

$$\boldsymbol{M}_k(t) = \frac{\lfloor kt \rfloor}{\sqrt{n}} \sum_{l=1}^{\lfloor kt \rfloor} \frac{1}{l} \psi(k|l)\boldsymbol{\zeta}_l, t \in [0,1],$$

and

$$\boldsymbol{B}_k(t) = \frac{1}{\sqrt{n}} \sum_{l=1}^{\lfloor kt \rfloor} \boldsymbol{\zeta}_l, t \in [0,1].$$

Proposition 2: Under the conditions of Proposition 1, $B_k(\cdot)$ converges weakly to a Brownian motion with mean 0 and covariance $\overline{\boldsymbol{S}}$, where $\overline{\boldsymbol{S}}$ is given by

$$\overline{\boldsymbol{S}} = E\boldsymbol{\zeta}_1\boldsymbol{\zeta}_1^{\mathrm{T}} + \sum_{j=2}^{\infty} E\,\boldsymbol{\zeta}_1\boldsymbol{\zeta}_j^{\mathrm{T}} + \sum_{j=2}^{\infty} E\,\boldsymbol{\zeta}_j\boldsymbol{\zeta}_1^{\mathrm{T}};$$

$\boldsymbol{M}_k(\cdot)$ converges weakly to $\boldsymbol{M}(\cdot)$ satisfying

$$\boldsymbol{M}(t) = \int_0^t \exp[-(\boldsymbol{I}-\boldsymbol{A})(\ln u - \ln t]\,\mathrm{d}\boldsymbol{B}(u).$$

The first assertion is a multidimensional extension of Theorem 7.3.1 in Ref. [17] and the second one follows from the first one by virtue of the following argument. A summation by parts in $\boldsymbol{M}_k(t)$ yields that

$$\boldsymbol{M}_k(t) = \boldsymbol{B}_k(t) + (\boldsymbol{I}-\boldsymbol{A})\lfloor kt\rfloor \sum_{j=1}^{\lfloor kt\rfloor} \frac{1}{j(j+1)}\psi(\lfloor kt\rfloor | j+1)\boldsymbol{B}_k\left(\frac{j}{k}\right).$$

The weak limit of the first term above tends to $B(t)$; the weak limit of the second term is the same as that of

$$(\boldsymbol{I}-\boldsymbol{A})\frac{1}{\lfloor kt\rfloor}\sum_{j=1}^{\lfloor kt\rfloor-1}\frac{\lfloor kt\rfloor^2}{j(j+1)}\exp\left[\boldsymbol{A}\ln\left(\frac{j+1}{kt}\right)\right]\boldsymbol{B}\left(\frac{j}{k}\right)\rightarrow$$

$$(\boldsymbol{I}-\boldsymbol{A})\int_0^1 \frac{1}{u^2}\exp(\boldsymbol{A}\ln u)\boldsymbol{B}(ut)\mathrm{d}u \quad \text{as } k \rightarrow \infty.$$

Hence,

$$\boldsymbol{M}(t) = \boldsymbol{B}(t) + (\boldsymbol{I}-\boldsymbol{A})\int_0^1 \frac{1}{u^2}\exp(\boldsymbol{A}\ln u)\,\boldsymbol{B}(ut)\mathrm{d}u.$$

Integrating by parts and making change of variable $ut \rightarrow u$, the desired theorem follows.

A corollary is $\sqrt{k}(\overline{\boldsymbol{S}}_{k+1}-\overline{\boldsymbol{S}}) \sim N(0,\boldsymbol{S})$, with $\boldsymbol{S}$ given by

$$\boldsymbol{S} = \int_0^{\infty} \exp\left(\frac{\boldsymbol{I}}{2}-\boldsymbol{A}\right)u\,\overline{\boldsymbol{S}}\exp\left(\frac{\boldsymbol{I}}{2}-\boldsymbol{A}\right)u\,\mathrm{d}u. \tag{7}$$

This is obtained by setting $t=1$ in $\boldsymbol{M}(t)$, evaluating $E\boldsymbol{M}(1)\boldsymbol{M}^{\mathrm{T}}$ (1) and making change of variable $u \rightarrow -\ln u$. A few details are omitted.

Since $\sqrt{k}(\overline{\boldsymbol{S}}_{k+1}-\overline{\boldsymbol{S}}) \sim N(0,\boldsymbol{S})$, if we can find a sequence $\boldsymbol{S}_k$ such that $\boldsymbol{S}_k \rightarrow \boldsymbol{S}$ and $\boldsymbol{S}_k^{-1}$ is non-singular, then

$$k(\boldsymbol{\theta}_{k+1}-\boldsymbol{\theta})^{\mathrm{T}}\boldsymbol{S}_k^{-1}(\boldsymbol{\theta}_{k+1}-\boldsymbol{\theta}) \overset{k}{\rightarrow} \chi_m^2$$

in distribution. Furthermore,

$$\boldsymbol{E}^k = \{k(\boldsymbol{\theta}_{k+1}-\boldsymbol{\theta})^{\mathrm{T}}S_k^{-1}(\boldsymbol{\theta}_{k+1}-\boldsymbol{\theta}) \leqslant c_\alpha\}$$

represents a ellipsoidal region and the volume of this region is given by

$$V(\boldsymbol{E}^k) = \frac{\pi^{\frac{m}{2}}\left(\frac{c}{k}\right)^{\frac{m}{2}}(\det \boldsymbol{S}_k)^{\frac{1}{2}}}{\Gamma\left(\frac{m}{2}+1\right)},$$

Where, $\Gamma(\cdot)$ denotes the Γ-function.

In view of the above paragraph, for any $\epsilon > 0$, we can choose $V(\boldsymbol{E}^k) \leqslant \epsilon^m$. Define

$$\gamma_\epsilon^k = \frac{\pi c_\alpha(\det \boldsymbol{S}_k)^{\frac{1}{m}}}{\epsilon^2\left[\Gamma\left(\frac{m}{2}+1\right)\right]^{\frac{1}{m}}};$$

$$\Lambda_\epsilon = \inf\{k;\gamma_\epsilon^k \leqslant k\}.$$

Define γ_ϵ as in γ_ϵ^k but with $\boldsymbol{S}_k$ replaced by $\boldsymbol{S}$. Λ_ϵ is the stopping rule. The desired limit theorem reads:

Proposition 3: If there exists a sequence $\{\boldsymbol{S}_k\}$, such that $\boldsymbol{S}_k \rightarrow \boldsymbol{S}$ a.s. with $\boldsymbol{S}$ given by Eq. (7), and if **(A1)**~**(A3)** are satisfied, then $\lim\limits_{\epsilon\rightarrow 0}\frac{\Lambda_\epsilon}{\gamma_\epsilon} = 1$ a.s.

$$\lim_{\epsilon\rightarrow 0} P\{\theta \in \boldsymbol{E}^{\Lambda_\epsilon} \text{ and } V(\boldsymbol{E}^{\Lambda_\epsilon}) \leqslant \epsilon^m\} = 1-\alpha.$$

By the definitions of γ_ϵ^k, γ_ϵ, and Λ_ϵ, the first assertion above is easily verified. As for the second assertion, we need only show that the stopped process is asymptotically normal, or put it another way, the asymptotic normality holds with deterministic time k replaced by the stopping time Λ_ϵ.

In the above, we have assumed an extra condition "if $\boldsymbol{S}_k$ exists and $\boldsymbol{S}_k \rightarrow \boldsymbol{S}$" . We demonstrate next that such $\boldsymbol{S}_k$ can be found. Define

$$\tilde{\boldsymbol{\zeta}}_k = \boldsymbol{\phi}_k z_k - \boldsymbol{\phi}_k\boldsymbol{\phi}_k^{\mathrm{T}}\boldsymbol{\theta}_k,$$

$$\boldsymbol{S}_k^i = \frac{1}{k}\sum_{j=1}^{k}\tilde{\boldsymbol{\zeta}}_j\tilde{\boldsymbol{\zeta}}_{j+i}^{\mathrm{T}}, i = 0,1,\cdots,k-1,$$

$$\tilde{\boldsymbol{S}}_k = \boldsymbol{S}_k^0 + \sum_{i=0}^{k-1}\left[\boldsymbol{S}_k^i + \left(\boldsymbol{S}_k^i\right)^{\mathrm{T}}\right].$$

By the ergodicity, it is fairly easy to see that $\tilde{\boldsymbol{S}}_k \rightarrow \overline{\boldsymbol{S}}$ a.s. as $k \rightarrow \propto$.

Next, define $\boldsymbol{S}_k$ by

$$\boldsymbol{S}_k = \int_0^{\infty}\exp[(\boldsymbol{I}/2-\boldsymbol{S}_k^0)t]\,\tilde{\boldsymbol{S}}_k\,[(\boldsymbol{I}/2-\boldsymbol{S}_k^0)t]\mathrm{d}t.$$

This definition is explicit. Nevertheless, as far as computation is concerned, such a formula may not be so attractive. We point out, however, that $\boldsymbol{S}_k$ can be constructed by solving the well-known Liapunov equation

$$\boldsymbol{S}_k(\boldsymbol{I}/2-\boldsymbol{S}_k^0) + (\boldsymbol{I}/2-\boldsymbol{S}_k^0)\boldsymbol{S}_k = -\tilde{\boldsymbol{S}}_k$$

recursively. The development provides an asymptotically accurate characterization of the confidence region and a stopping rule on the estimates.

4 Projection Algorithms

In practice, when recursive algorithms are implemented, one often uses some kind of truncation or projection algorithms to ensure boundedness of certain signals and states. The idea is that the iterate is projected back to some finite set if it leaves it.

In this section, several projection algorithms for the supervised learning were discussed, without detailed proofs. Pertinent references were given for further details on rigorous treatments.

4.1 A box Projection Region

The following algorithm was introduced in Ref. [18], later studied thoroughly in Ref. [19] and [20] for adaptive filtering problems. We adopt their ideas for this analysis.

Let θ^i be the ith component of $\boldsymbol{\theta}$ and similarly for $\boldsymbol{\theta}_k^i$. Suppose that we have some knowledge about where the optimal vector $\boldsymbol{\theta}$ lies. We may modify our supervised learning algorithm as follows. Let $G = \{x; |x^i| \leqslant \eta\}$ for some positive real number η. If some $|\boldsymbol{\theta}_k^i| > \eta$, then θ_k^i is immediately reset to the closest value η or $-\eta$. Ljung's version of the algorithm requires that $\boldsymbol{\theta}$ be strictly inside the box G. Kushner generalized this by allowing $\boldsymbol{\theta}$ to be either in the interior or on the boundary.

For any x, let $\pi_G(x)$ denote the nearest point on G to x. Then the projection algorithm can be written as

$$\begin{aligned}\tilde{\boldsymbol{\theta}}_{k+1} &= \boldsymbol{\theta}_k - \frac{1}{k}\left(\boldsymbol{\varphi}_k\boldsymbol{\varphi}_k^{\mathrm{T}}\boldsymbol{\theta}_k - \boldsymbol{\varphi}_k z_k\right),\\ \boldsymbol{\theta}_{k+1} &= \pi_G\left(\tilde{\boldsymbol{\theta}}_{k+1}\right).\end{aligned} \tag{8}$$

It can be shown that under appropriate conditions, $\boldsymbol{\theta}_k$ given by Eq.(8) converges a.s. to the closest point $\pi_G(\boldsymbol{\theta})$ in G to $\boldsymbol{\theta}$, the optimal vector.

4.2 A more General Projection Algorithm

Let $g_i(\cdot)$, $i \leqslant s$ be continuously differentiable functions and define $L=\{x; g_i(x) \leqslant 0, i=1,\cdots,s\}$. Let L be bounded and closure of its interior unless $g_i(\cdot)$ is linear. Suppose $\nabla g_i(x) \neq 0$ if $g_i(x) = 0$, i.e., $g_i(x)$ has only simple zeros. Let $\pi_L(x)$ denote the closest point in L to x. A projection algorithm with respect to the set L is of the same form as (8) with π_G replaced by π_L. Similar convergence analysis can be carried out. The study of the convergence properties can also be connected with the *Kuhn-Tucker* point (see Ref. [20] for instance).

4.3 Randomly Varying Projections

Such an approach was first developed in Ref. [17] for Robbins-Monro (RM) algorithms and was further generalized to treat stochastic approximations with non-additive noise in our recent work[18]. In this approach, no *a priori* information on the region where $\boldsymbol{\theta}$ belongs is needed. A sequence of random truncation bounds is generated recursively, and the iterates are compared with the truncation bound at each step. If the iterate exceeds the bound, then it is projected back to a fixed but otherwise arbitrary point; else the iterate is computed as in the usual case. Let $\boldsymbol{M}(k)$ be a sequence of increasing positive real numbers. The algorithm can be written as:

$$\tilde{\boldsymbol{\theta}}_{k+1} = \boldsymbol{\theta}_k - \frac{1}{k}\left(\boldsymbol{\varphi}_k\boldsymbol{\varphi}_k^{\mathrm{T}}\boldsymbol{\theta}_k - \boldsymbol{\varphi}_k z_k\right), \tag{9}$$

$$\sigma_k = \sum_{j=1}^{k-1} I_{\{|\tilde{\boldsymbol{\theta}}_{j+1}| > M(\sigma_j)\}}, \tag{10}$$

$$\boldsymbol{\theta}_{k+1} = \tilde{\boldsymbol{\theta}}_{k+1} I_{\{|\tilde{\boldsymbol{\theta}}_{k+1}| \leq \boldsymbol{M}(\sigma_k)\}} + \boldsymbol{\theta}^* I_{\{|\tilde{\boldsymbol{\theta}}_{k+1}| > \boldsymbol{M}(\sigma_k)\}}. \tag{11}$$

It can be shown that $\sigma_k \overset{k}{\to} \sigma < \propto$, and hence the iterates are eventually bounded. Moreover, it can be shown that the strong consistency holds in that $\boldsymbol{\theta}_k \to \boldsymbol{\theta}$ a.s.

Remark 2: The box projection algorithm has the simplest form. This kind of algorithms has been widely used. However, for the other two bounding algorithms, some prior information on $\boldsymbol{\theta}$ is needed. If the situation is completely unknown, they cannot be applied. The main advantage of the varying projections is that the *a priori* knowledge on $\boldsymbol{\theta}$ is not needed. In addition, the first two algorithms converge a.s. to $\pi_G(\boldsymbol{\theta})$ or $\pi_L(\boldsymbol{\theta})$, the closest point to $\boldsymbol{\theta}$ in G or L respectively (if $\boldsymbol{\theta}$ is in the interior of G or L, $\pi_G(\boldsymbol{\theta}) = \boldsymbol{\theta}$ resp. $\pi_L(\boldsymbol{\theta}) = \boldsymbol{\theta}$). For the random truncation algorithm, $\boldsymbol{\theta}_k$ converges a.s. to $\boldsymbol{\theta}$.

5 A Case Study

To illustrate the results of this paper, we considered an electric vehicle that followed another vehicle in front of it. The front vehicle kept a cruising speed for a period of time and then accelerated to a new cruise speed. The goal of the autonomous vehicle's control was to follow the front vehicle and also kept a desired safe distance.

The following simplified yet representative vehicle dynamic models from Ref. [21] was used as a benchmark case

$$\dot{d} = v_{\mathrm{ref}} - v, \quad m\dot{v} + c(v) = f\,. \tag{12}$$

where v is the vehicle speed, m is the consolidated vehicle mass (including the vehicle, passengers, etc.). The resistance force term $c(v)$ represents gravitational pull (uphill), aerodynamic drag and frictions. The net driving force f acts on the vehicle's gravitational center. We use the typical form of $c(v) = a_0 + a_1 v + a_2 v^2$, where $a_0 > 0$ is the tire rolling resistance, a_1 is the linear friction coefficient, and $a_2 > 0$ is the aerodynamic drag coefficient. These parameters depend on many factors such as the vehicle weight, exterior profile, tire types and aging, road conditions, wind strength and directions. Consequently, they are usually determined experimentally and approximately.

For simplicity, we ignore the actuator dynamics and control f directly.

$$\dot{v} = \frac{f}{m} \quad - \frac{a_0 + a_1 v + a_2 v^2}{m}.$$

The observations are noise corrupted, leading to $\hat{v}_k = v_k + \epsilon_k^v$, $\hat{d}_k = d_k + \epsilon_k^d$, where ϵ_k^v and e_k^d are i.i.d. processes of mean [21] and finite variances.

The feedback is

$$f = \gamma_{\mathrm{d}}\left(\hat{d} - d_{\mathrm{ref}}\right) + \gamma_{\mathrm{v}}(v_{\mathrm{ref}} - \hat{v})\,,$$

where γ_{d} and γ_{v} are the control gains. Since it is common to use $a_1 = 0$ in the auto industry, this is adopted in this case study. The closed-loop system can be written as

$$\dot{v} = \frac{1}{m}\left[\gamma_{\mathrm{d}}\left(\hat{d} - d_{\mathrm{ref}}\right) + \gamma_{\mathrm{v}}(v_{\mathrm{ref}} - \hat{v})\right] - \frac{a_0 + a_2 v^2}{m}. \tag{13}$$

Select a sampling interval τ second. The sampled system of Eq. (13) is

$$v_{k+1} = v_k + \tau\left[\frac{\gamma_{\mathrm{d}}}{m}\left(\hat{d} - d_{\mathrm{ref}}\right) + \frac{\gamma_{\mathrm{v}}}{m}(v_{\mathrm{ref}} - \hat{v}) - \frac{a_0 + a_2 v^2}{m}\right]. \tag{14}$$

For system identification, this can be put into a regression form

$$y_k = \boldsymbol{\Phi}_k^{\mathrm{T}}\boldsymbol{\theta}\,,$$

Where, $y_k = v_{k+1} - v_k$; $\boldsymbol{\Phi}_k^{\mathrm{T}} = \left[\tau\left(\hat{d}_k - d_{\mathrm{ref}}\right), \tau\left(v_{\mathrm{ref},k} - \hat{v}_k\right), -\tau, -\tau v_k^2\right]$, and $\boldsymbol{\theta} = \left[\frac{\gamma_{\mathrm{d}}}{m}, \frac{\gamma_{\mathrm{v}}}{m}, \frac{a_0}{m}, \frac{a_2}{m}\right]^{\mathrm{T}}$. Since m is unknown, we have grouped it into the unknown parameters. Also, in consideration of potential impact of communication systems, actuator uncertainties on the control gains, γ_d and γ_v are also treated as unknown variables.

For our simulation study, we used some modified parameters from Ref. [21]. Under the MKS (metre, kilogram, second) system of units, the vehicle mass m has the range 1.2 ~ 1.5 t; a_0 has the range 0.005 ~ 0.025 kg·m/s^2, and the aerodynamic drag coefficient a_2 has the range 0.35 ~ 2.1 kg/m, depending on wind and road conditions. For example, strong head wind and uphill driving will have much more resistance than those on flat road and low wind speed conditions.

We will used m = 2 t, a_0 = 0.01, and a_2 = 0.43 as the true parameters. The true feedback gains are γ_d = 1 500 and γ_v = 3 000. The desired inter-vehicle distance d_{ref} = 60 m, which is about 3-second distance under 72.4 km/h. The cruising speed is initially v_{ref} = 80.5 km/h and then increases to 96.6 km/h. The observation noise ϵ_k^d is i.i.d., mean zero and standard deviation 0.4; and ϵ_k^v is i.i.d., mean zero and standard deviation 0.2.

The sampling interval is τ = 10 ms. The vehicle's speed and distance responses to the change of v_{ref} are depicted in Figure 2.

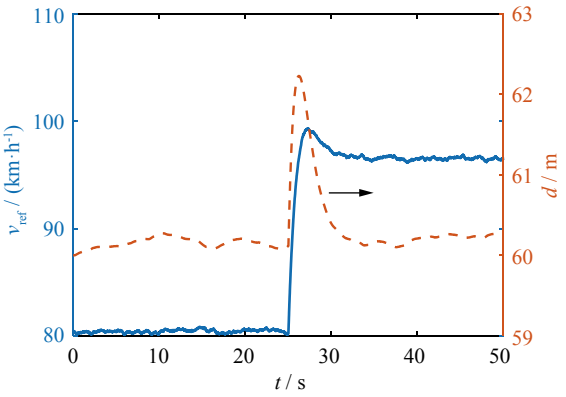

Figure 2 Speed and Distance Trajectories after an Acceleration of the Front Vehicle

Due to ever-changing operating conditions, the vehicle parameters m, a_0, a_2, γ_d, γ_v may change with time. Consequently, it is desirable to adapt the controllers to achieve a better balance among the peak power (to reduce discharge current rate for battery health), total energy per maneuver (for better fuel economy), and distance deviations (for safety and highway space utility). System identification during operation becomes important.

As a result, we used observation data on d and v to estimate θ and characterize identification accuracy and reliability in this case study. The total duration of data acquisition was 50 s, hence 3 000 noise-corrupted data points were collected.

In this case study, it is noted that a_0 is small, independent of the vehicle speed, and has very limited impact on control design. As a result, we focued on the estimates for $c_0 = \frac{\gamma_{\mathrm{d}}}{m}$, $c_1 = \frac{\gamma_{\mathrm{v}}}{m}$, $c_3 = \frac{a_2}{m}$.

To characterize estimation errors, the simulation was repeated 3 000 times under the same operating conditions. Estimates for the parameters c_0, c_1, and c_3 are depicted as histograms in Figure 3. Their means and variances are listed in Table 1. From these parameters, it is easy to derive sample confidence intervals on the parameters.

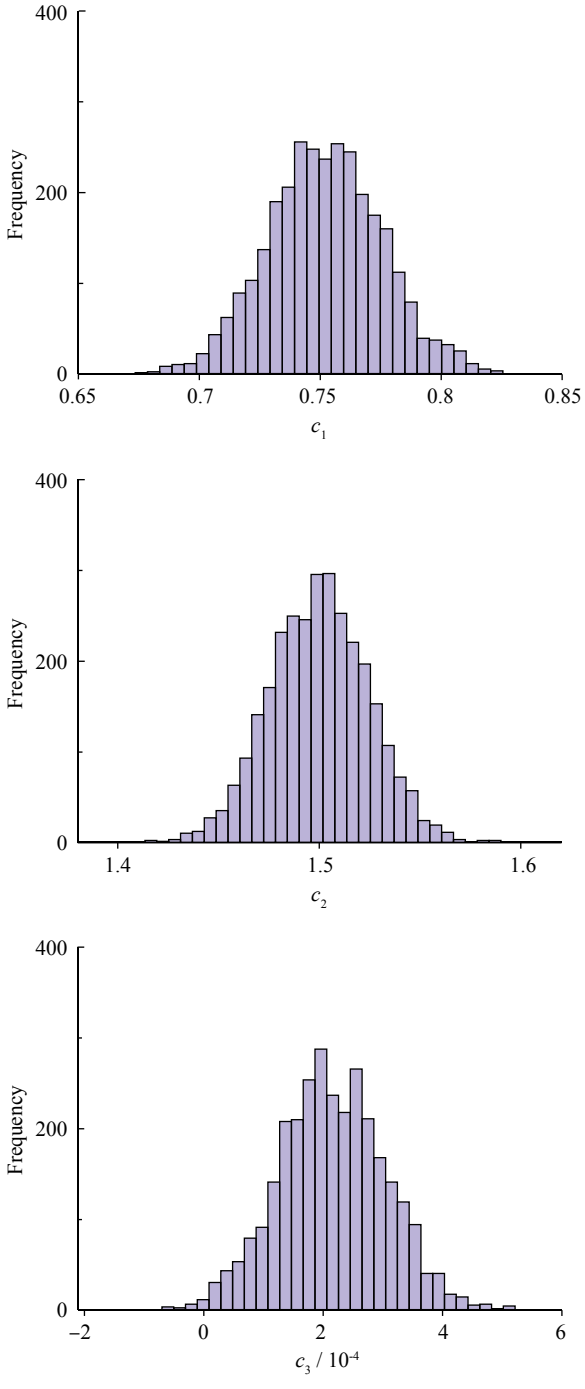

Figure 3 The Histograms of the Estimates of c_0, c_1, and c_3.

Table 1 Means and Variances of the Estimates

Estimate	c_0	c_1	c_3
True value	0.750 0	1.500 0	$2.150\ 0\times10^{-4}$
Sample mean	0.751 4	1.500 2	$2.152\ 4\times10^{-4}$
Sample variance	$5.303\ 8\times10^{-4}$	$5.682\ 1\times10^{-4}$	$7.291\ 9\times10^{-4}$

To make the errors comparable and scalable, in calculating the total errors, we used the relative mean-square errors

$$e=\left(\frac{\hat{c}_1-c_1}{c_1}\right)^2+\left(\frac{\hat{c}_2-c_2}{c_2}\right)^2+\left(\frac{\hat{c}_3-c_3}{c_3}\right)^2.$$

The empirical error distributions are depicted by the histogram in Figure 4. It can be seen that the shape resembles a (folded to the positive side) Gaussian distribution.

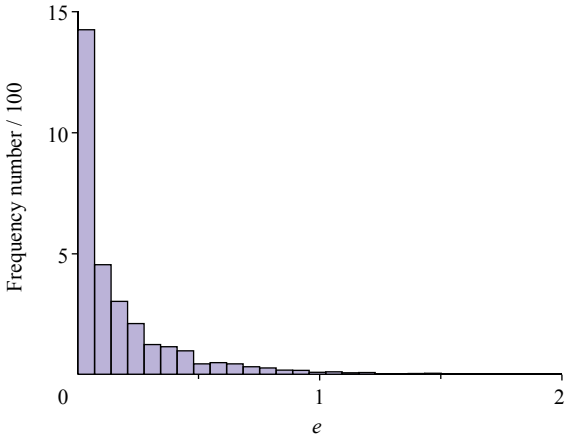

Figure 4 The Histogram of the Relative Mean−Square Errors from 3 000 Repeated Evaluations on Estimated Parameters

6 Concluding Remarks

This paper is focused on a basic scenario of an autonomous vehicle following its front vehicle. By using recursive algorithms and confidence ellipsoid characterization of parameter estimates, this paper studies algorithms and their features such that vehicle control performance can be quantified in a stochastic framework. A simulation case study is used to illustrate the strategies of which results show the proposed method can estimate the vehicle's parameters accurately. The findings of the paper can potentially lead to useful data-driven controller tuning methods for control of autonomous vehicles.

References / 参考文献

[1] Xu S, Li S E, Cheng B, et al. Instantaneous feedback control for a fuel-prioritized vehicle cruising system on highways with a varying slope [J]. ***J IEEE Trans Intell Transp Syst***, 2017, **18**(5): 1210-1220.

[2] Zheng Y, Li S E, Li K, et al. Distributed model predictive control for heterogeneous vehicle platoons under unidirectional topologies [J]. ***IEEE Trans Control Syst Tech***, 2017, **25**(3): 899-910.

[3] Li S E, Li R, Wang J, et al. Stabilizing periodic control of automated vehicle platoon with minimized fuel consumption [J]. ***IEEE Trans Trans Electrification***, 2017, **3**(1): 259-271.

[4] Rajamani R, Tan H S, Law B, et al. Demonstration of integrated lateral and longitudinal control for the operation of automated vehicles in platoons [J]. ***IEEE Trans Control Syst Tech***, 2000, **8**(4): 695-708.

[5] Liang Y, Peng H, String stability analysis of adaptive cruise controlled vehicles [J]. ***JSME Int J C***. 2000, **43**(3): 671-677.

[6] Hsu H C and Liu A. Kinematic design for platoon-lane-change maneuvers [J]. ***IEEE Trans Intell Transp Syst***, 2008, **9**(1): 185-190.

[7] Alam N, Dempster A G, Cooperative positioning for vehicular networks: facts and future [J]. ***IEEE Trans Intell Transp Syst***, 2013, **14**(4): 1708-1717.

[8] Wang L Y, Syed A, Yin G, et al. Control of vehicle platoons for highway safety and efficient utility: Consensus with communications and vehicle dynamics [J]. ***J Syst Sci Complex***, 2014, **27**(4): 605-631.

[9] Gao F, Li S E, Zheng Y, et al. Robust control of heterogeneous vehicular platoon with uncertain dynamics and communication delay [J]. ***IET Intell Transp Syst***, 2016, **10**(7): 503-513, 2016.

[10] Li S E, Guo Q, Xin L, et al. Fuel-saving servo-loop control for an adaptive cruise control system of road vehicles with step-gear transmission [J]. ***IEEE Trans Vehi. Tech***, 2017, **66**(3): 2033-2043.

[11] Li S E, Qin X, Li K, et al. Robustness analysis and controller synthesis of homogeneous vehicular platoons with bounded parameter uncertainty [J]. ***IEEE/ASME Trans Mechatronics***, 2017, **22**(2): 1014-1025.

[12] Chen H F. Recursive Estimation and Control of Stochastic Systems [M]. Wiley, New York, 1985.

[13] Zhu Y M, Yin G. Adaptive filter with constraint and correlated nonstationary signals [J]. ***Syst Control Lett***, 1988, **10**: 271-279.

[14] Chow Y S and Robbins R. On the asymptotic theory of fixed-width sequential confidence intervals [J]. ***Ann Math Statist***, 1965, **36**: 457-462.

[15] Yin G. A stopping rule for least squares identification [J]. ***IEEE Trans Autom Contr***, 1989, **AC-34**：659-662.

[16] Yin G. A stopping rule for the Robbins-Monro method, to appear [J]. ***J Optim Theory Appl***, 1990, **67**(1): 151-173.

[17] Ethier S N and Kurtz T G. Markov Processes, Characterization and Convergence [M]. Wiley, New York, 1986.

[18] Ljung L. Analysis of recursive stochastic algorithms [J]. ***IEEE Trans Autom Contr***, 1977, **AC-22**: 551-575.

[19] Kushner H. A projected stochastic approximation method for adaptive filters and identifications [J]. ***IEEE Trans Autom Contr***, 1980, **AC-25**: 836-838.

[20] Kushner H, Approximation and Weak Convergence Methods for Random Processes, with applications to Stochastic Systems Theory [M]. MIT Press, 1984.

[21] McMahon D H，Hedrick J K, Shladover S E. Vehicle modelling and control for automated highway systems [C] // *Proc Amer Contr Conf.* San Diego CA, USA, 1990: 297-303,